Bulk superconductivity in both tetragonal and orthorhombic solid solutions of $(La_{1-x}Sr_x)_2CuO_{4-\delta}$

T. Nagano, Y. Tomioka, Y. Nakayama, K. Kishio, and K. Kitazawa
Department of Industrial Chemistry, University of Tokyo, 7-3-1 Hongo, Bunkyo-ku, Tokyo 113, Japan
(Received 19 March 1993; revised manuscript received 24 June 1993)

Comparative measurements of low-field Meissner and shielding signals of both powder and sintered pellet samples of $(La_{1-x}Sr_x)_2CuO_{4-\delta}$ have revealed that bulk superconductivity is present over a wide range of Sr composition, $0.0425 \leq x \leq 0.125$, extending over the orthorhombic-to-tetragonal phase boundary at $x \cong 0.105$, except for a narrow anomaly region $x = 0.0625$. Samples were prepared by three different methods through a combination of spray-drying or powder-mixing preparation with either slow cooling or quenching from the sintering temperature of 1100 °C down to 500 °C, at which oxygenation annealing was performed. Homogeneous solid solutions were obtained only for specimens prepared by spray drying and slow cooling. Dependences of the Meissner and shielding signals on the Sr content, on the intensity of magnetic field, and on the sample size were examined in terms of pinning effect and penetration depth.

I. INTRODUCTION

In cuprates, superconductivity manifests itself on doping of holes or electrons in the host insulative materials. This implies that superconductivity is usually observed in compounds with nonstoichiometric composition, that is, in "solid-solution" systems.[1,2] According to thermodynamics, any solid-solution system in principle must undergo phase separation at low enough temperatures. In this context, all actual solid-solution samples should be regarded as quenched and thus, thermodynamically unstable. In order to study superconducting properties as a function of the composition, therefore, it is essential to know whether the actual samples of a cuprate solid-solution system are homogeneous from the aspect of superconductivity. Jorgensen *et al.*[3] reported a phase instability to occur in $(La_{1-x}Sr_x)_2CuO_4$ (LSCO) at $0.075 \leq x \leq 0.20$ due to the miscibility gap in this compositional region according to neutron-diffraction measurement. Yoshimura *et al.*[4] proposed that the superconductivity in this system occurs in a very limited compositional region near $x = 0.080$ with fully oxygenated samples, based on their ac susceptibility measurement. They considered that the continuous suppression of T_c on both sides of the optimum composition of $x = 0.080$ was caused by the proximity effect between the superconducting phase ($x = 0.080$) and the nonsuperconducting secondary phase with $x \neq 0.080$. Similar views have been shared by other researchers from the early period of the studies on high-temperature superconductivity.[5,6] If such a phase separation is unavoidable in practical cuprate solid-solution systems, many efforts conducted so far to relate various superconductivity parameters as a function of the composition (or hole concentration) would become meaningless.

On the other hand, there is another aspect in regard to the criterion of the homogeneity of the solid-solution system, the relevant length scale. On the scale of atomic size, for example, the number of nearest-neighbor Sr or La sites around each Cu atom is 8. Therefore, even in the ideal solid-solution system of LSCO, the number of nearest-neighbor Sr ions around a given Cu site can discretely vary from 0 through 8. If the analytical probe we use senses the environment on the length scale of nearest neighbors, this system will turn out to be a mixture of nine different phases. But if the length scale is longer, say more than a few nanometers, this system will then appear to be homogeneous. In this context, we must decide on a length scale to discuss the homogeneity of a solid-solution system. Yoshimura *et al.*[7] observed the presence of three nonequivalent Cu nuclear quadrupole resonance (NQR) peaks at which the relative intensities change with Sr/La ratio. This observation, however, does not necessarily mean that the system was phase separated nor that it was inhomogeneous in terms of superconductivity. The order parameter varies with the characteristic length scale of the coherence length ξ which is, typically, a few nanometers. So a superconductor may be homogeneous even if the sample is judged inhomogeneous by a probe with a shorter length scale.

As a probe to judge the superconducting volume fraction of a sample, the intensity of the Meissner signals has often been used. However, it has been pointed out that the Meissner fraction tends to significantly underestimate the true superconducting volume fraction unless measurements are made under very low magnetic fields, such as 0.1 Oe.[8–10] Furthermore, it has been found that the observed value depends also on the sample size; the larger sample exhibits the smaller Meissner fraction.[10] Besides, the Meissner fraction is subjected to the presence of weak links associated with the polycrystalline samples.[11,12] These findings have been quantitatively explained in terms of the pinning effect of vortices during the field cooling process.[13,14] As an example, the observed Meissner volume fraction was only 2% for a single-crystal LSCO specimen of thickness 0.7 mm under a measurement field of 10 Oe, a typical field value often employed, while it improved to essentially 100% when the sample thickness was reduced to 0.2 mm and measured under a much reduced field of 0.1 Oe (Ref. 10). Therefore, one

should realize that the Meissner signal could lead to a serious underestimation of the fraction of superconductivity.

It has been frequently argued that a solid-solution oxide system, such as LSCO, is composed of inhomogeneous mixtures of a superconducting ordered phase of a certain composition and other nonsuperconducting phases.[5,6] On the other hand, Takagi *et al.*[15] have reported that LSCO is a homogeneous solid solution in both the orthorhombic and tetragonal phase regions, but that it is essentially nonsuperconductive in the tetragonal phase region. Considering the above-discussed characteristics of the Meissner effect, these results should be reexamined by paying attention to the factors which can influence the observed Meissner fraction. Also, evaluation of the superconducting volume fraction by some other independent method would be necessary.

In this paper, we report a systematic examination of the superconducting volume fraction by both Meissner and shielding effects under various magnetic fields on samples of various sizes. We propose that there is a suitable processing method to obtain homogeneous superconducting solid-solution samples of LSCO over a much wider composition range, $0.0425 \leq x \leq 0.125$, than the previously reported composition range. The bulk superconductivity region extends both over the tetragonal ($0.105 \leq x$) and orthohombic phase regions.

II. EXPERIMENT

In order to differentiate between the possible origins of the compositional inhomogeneity, the LSCO samples were prepared using three different processes. Starting materials were mixed either conventionally in an agate mortar and pestle using La_2O_3, $SrCO_3$, and CuO, or by a solution route. In the latter, starting materials La_2O_3, $SrCO_3$, and $Cu(CH_3COO)_2$ were separately dissolved into acetic acid solutions and a prescribed amount of each solution was mixed after chemical titration to examine the compositional ratio. The mixed liquid was dried at 140 °C in commercial spray-drying equipment in a cyclone-air stream (Yamato Science, Ltd.) and the obtained powder was further heated to 400 °C in air. The resulting powders from both routes were calcined at 950 °C for 12 h in air and cooled to room temperature at a rate of 2 °C/min. These powders were ground and pressed into pellets and heated at 1100 °C for 90 h in a flowing pure oxygen atmosphere and cooled down to 500 °C at a rate of 0.1 °C/min. They were then annealed at 500 °C for 90 h and further at 400 °C for 150 h, followed by slow cooling at a rate of 0.1 °C/min down to room temperature in order to assist the oxygen loading. Some of the spray-dried samples were quenched from 1100 °C to 500 °C, but otherwise the identical slow cooling heat treatment was given below 500 °C. The samples prepared by the three different processing methods here are denoted as "spray-dried–slow-cooled," "spray-dried–quenched," and "powder-mixed–slow-cooled".

Prepared samples were characterized with an x-ray diffractometer equipped with a rotating Cu anode (40 kV, 150 mA). Low-temperature x-ray-diffraction patterns were obtained at 10 K using the same apparatus. Evaluations of the μm range inhomogeneity and grain sizes of the samples were performed using an electron probe microanalyzer (EPMA), JEOL, JXA-8621. Resistivity was measured by the standard four-probe method with the aid of silver paste electrodes. Oxygen content was determined by the iodometric titration technique.[16] A 200–300 mg weight of sample was used for each titration and ten measurements were averaged to get the datum for each composition. The error in δ was about $\Delta\delta = 0.001$ or less in the formula $(La_{1-x}Sr_x)_2CuO_{4-\delta}$. Shielding and Meissner signals were measured with a superconducting quantum interference device (SQUID) susceptometer (Hoxan Co., HSM-2000X) on both powdered samples and pelletized rectangular block samples of $8.0 \times 1.5 \times 0.5$ mm^3. Various fields of 10, 1.0, 0.2, and 0.05 Oe were applied along the longest edge of the rectangular block in order to minimize the demagnetization effect. The inside of the coil was equipped with a niobium superconducting shield tube in order to stabilize the field during the measurements. The applied field was calibrated with the aid of the standard Pb superconducting sample at 4.2 K. Magnetization in the vicinity of T_c was measured under 0.1 T with the same equipment. Equilibrium magnetization was measured under 0.1 ~ 1T with another SQUID (Quantum Design, MPMS).

III. RESULTS AND DISCUSSION

A. Chemical homogeneity of samples

In all the LSCO samples prepared in this work, no secondary phase was detected by x-ray diffraction (XRD) over the whole composition range $0.025 \leq x \leq 0.15$. Lattice parameters changed continuously with increasing Sr content. The scanning electron microscopy (SEM) image of the polished surface of the sintered specimens showed that the grain size was 10–50 μm and porosity was less than 10% in the spray-dried samples. On the other hand, in powder-mixed samples porosity was more than 20%. Quantitative and mapping composition analyses by EPMA indicated that no detectable inhomogeneity of the cation distribution was present within the resolution length limit of 1 μm.

Figure 1 shows chemically analyzed oxygen content in the samples by the three different processing methods. It is noted that the spray-dried–slow-cooled samples are nearly fully oxygen loaded, while the other two methods lead to oxygen deficiency even though they were oxygenated for prolonged periods at temperatures below 500 °C with the conditions described in the experimental section. Figure 2 shows the full width at half maximum (FWHM) of the main peak (103) of the three series of samples. All spray-dried samples have a FWHM of about $(0.115 \pm 0.005)°$ over the whole range of the Sr content while that of powder-mixed samples have larger values, except at $0.075 \leq x \leq 0.105$. Although a sizeable oxygen deficiency was observed in spray-dried–quenched samples but not in spray-dried–slow-cooled samples, there were no clear differences in the FWHM between the two series of samples. This indicates that the remarkable

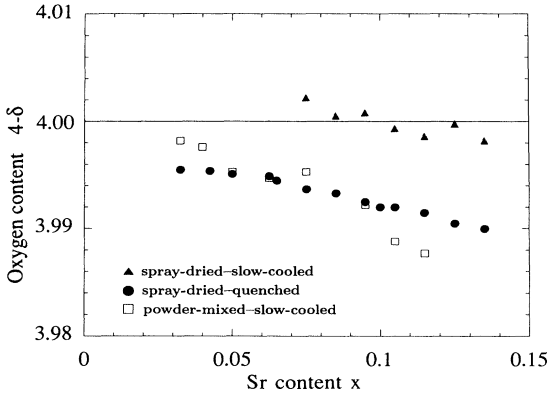

FIG. 1. Oxygen content measured by iodometric titration of $(La_{1-x}Sr_x)_2CuO_{4-\delta}$ prepared by three different methods.

broadening of the FWHM in powder-mixed samples should be related to the compositional fluctuation of Sr, but not to that of oxygen content. Therefore, we can conclude that Sr distribution is inhomogeneous in the powder-mixed samples except at $0.075 \leq x \leq 0.105$ over the length scale detectable by XRD, being estimated at about a few tenths of a nanometer.

Figure 3 shows the resistivity and magnetization curves near T_c for the three series of samples. As is typically shown in Fig. 3(c-3), a two-step-like transition is seen in the overdoped region for the powder-mixed–slow-cooled samples. The first step is always seen at 40 K independent of the composition, whereas the second step appears at gradually decreasing temperature as x is increased. This clearly indicates the presence of two phases of which one always has an onset T_c of 40 K, while the other T_c is variable. The susceptibility results in Fig. 3(c-1) are presented in order to show the susceptibility onset temperature under a rather elevated magnetic field of 1000 Oe for better sensitivity. In this figure, the onset at 40 K can also be seen, except at $x = 0.050$. The

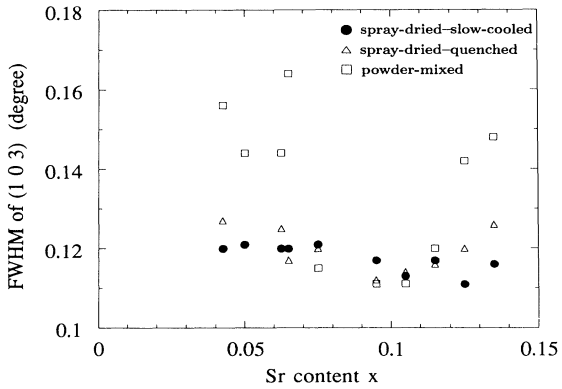

FIG. 2. The full width at half maximum height (FWHM) of (103) XRD peak of samples prepared by three different methods. Almost constant values of 0.115±0.005° are observed for all spray-dried samples.

two-step-like transitions with the onset at 40 K have been frequently observed in these powder-mixed specimens especially clearly in the overdoped region $x > 0.075$.

The similar two-step-like transitions are also observed, though to a lesser extent, in Figs. 3(b-1) and 3(b-3) for the spray-dried–quenched samples, indicating that this series of samples is also subjected to a slight phase separation. It should be noted that the 40 K phase is only present in the overdoped region ($x > 0.075$) for the spray-dried–quenched samples.

In Fig. 3(a), in contrast to the previous results, both the resistivity and susceptibility curves are well defined by a single T_c value for each composition. T_c varies continuously with Sr content, increasing in the underdoped region ($x < 0.075$) and decreasing in the overdoped region ($x > 0.075$). This series of samples does not have a significant amount of oxygen deficiency. These observations indicate the homogeneous distribution of Sr both in the underdoped and overdoped regions as far as it is judged over the characteristic length scale of superconductivity. The coherence length ξ_0 in LSCO is known to be about 30 Å in the *ab* plane.[17,18]

With the aid of a nuclear quadrupole resonance (NQR) probe, Yoshimura *et al.*[7] reported that the environment of Cu did not change continuously with the Sr content, but, rather, they observed the two peaks at which the relative spectral weight changed with composition. From this result, they suggested that phase separation occurred in the overdoped region. However, we presume that the NQR technique in their case probed the atomic length scale. If so, even an ideal solid solution would give rise to signals of Cu atoms in distinctive environments. It should, therefore, be noted that a solid solution can appear to be homogeneous with respect to one definition (e.g., superconductivity) but inhomogeneous with another (e.g., NQR).

In the remaining part of this paper, we will confine our discussion only to a spray-dried–slow-cooled series of samples because the above arguments tell us that the samples obtained can be regarded as homogeneous in terms of superconductivity.

B. Superconducting volume fraction

In the spray-dried–slow-cooled samples, the superconducting transition was well defined and the T_c changed continuously, going up in the underdoped region and coming down in the overdoped region with increase in the Sr content. There are two standard magnetic methods to evaluate the superconducting volume fraction: the Meissner effect and the shielding effect. However, the former tends to underestimate, while the latter may overestimate the superconducting volume fraction. This is because in the field cooling process, the Meissner effect can be incomplete due to the residual flux lines trapped in the sample by flux pinning. On the other hand, the flux expulsion may still be perfect even when a nonsuperconducting region is surrounded by a superconducting region if the field is applied after the sample cooling (shielding effect). Therefore, caution must be exercised when judging the superconducting volume fraction

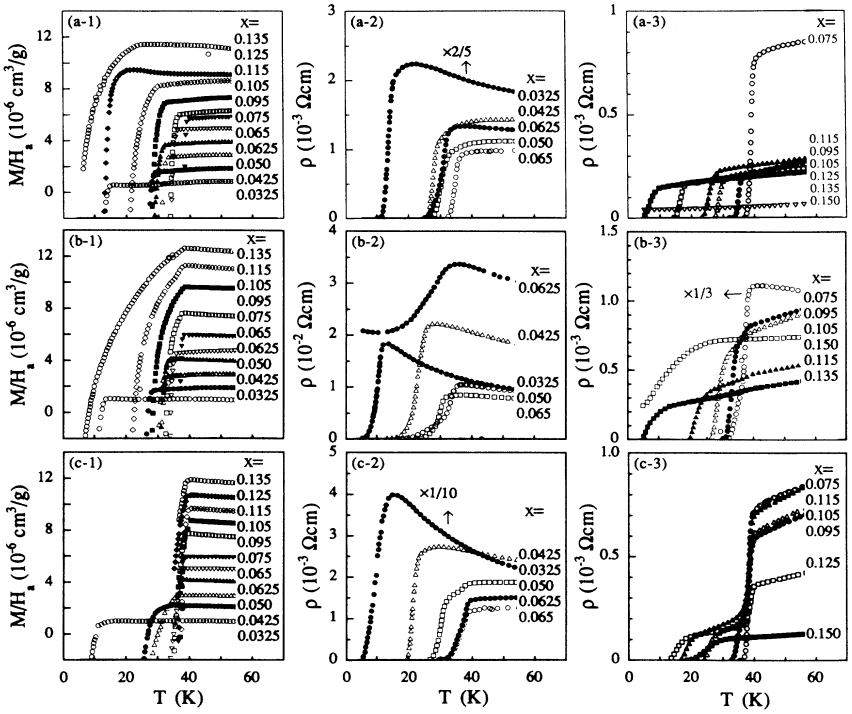

FIG. 3. Temperature dependences of reversible magnetization in the superconductivity onset region (1), resistivity in the underdoped region (2), and resistivity in the overdoped region (3), for (a) spray-dried–slow-cooled, (b) spray-dried–quenched, and (c) powder-mixed–slow-cooled samples, respectively. The numbers in the figure correspond to the composition x. Magnetization curves were obtained under $H_a = 1000$ Oe as temperature was decreased. Each M/H curve is arbitrarily shifted vertically except the bottom one for clarity. Note that the well-defined superconducting transitions are obtained only in the series of (a) in the overdoped region. The composition $x = 0.0625$ is related with a structural anomaly described in the text. Some of the curves are reduced in magnification for clarity.

from these measurements.

Figure 4 shows the temperature dependences of the magnetization of sintered pelletized samples under a small applied magnetic field, $H_a = 0.2$ Oe. The warming curves represent the shielding effect or zero-field cooling process, and the cooling curves represent the Meissner effect or field cooling processes. The superconducting volume fractions estimated from two types of measurements at 4.2 K under various magnetic fields are illustrated in Figs. 5(a) and 5(b), respectively.

First of all, we would like to point out a distinct anomaly seen in the sample for $x = 0.0625$. For this composition, the shielding signal reaches only about 50%, while the Meissner signal is approximately 33% of full volume fraction. The former is much smaller and the latter is larger when compared to the signals for the neighbor compositions $x = 0.050$, 0.065, and others. Going back to Fig. 4, the transition width and the reversible temperature range are seen to be much larger than for the other compositions. These observations suggest that $x = 0.0625$ $(= 1/16)$ corresponds to the well-established special composition in the $(La_{1-x}Ba_x)_2CuO_{4-\delta}$ system, where a structural anomaly and the disappearance of superconductivity have been reported.[19,20] However, the composition range for which this anomaly appears seems to be much narrower in the present system. From powder-x-ray diffraction at 10 K, we could not detect any structural change in the present composition $x = 0.0625$, in contrast to the $(La_{1-x}Ba_x)_2CuO_{4-\delta}$ which transforms to a low-temperature tetragonal phase.[20] In spite of this, the low shielding fraction as indicated in Fig. 5(a) clearly shows that the sample lacks its full bulk superconductivity at this particular composition in $(La_{1-x}Sr_x)_2CuO_{4-\delta}$.

Except for this special composition, all the samples over the compositional range $0.0425 \le x \le 0.125$ show 102–110% of shielding volume fraction (-1.14×10^{-2} cm^3/g corresponds to the perfect superconducting volume fraction of the material with $x = 0.075$). The reason why it slightly exceeds 100% can be attributed to the demagnetization effect, ~2% at most, and the sample porosity of about several percent. When the applied field is raised to 10 Oe, the shielding signal becomes significantly smaller. This can be explained by assuming the penetration of vortex lines along the weak links at grain boundaries. It is evident that the Meissner volume fraction is significantly smaller than the shielding volume fraction under the present experimental conditions. Here we tentatively assume that the shielding volume fraction, essentially 100%, represents the real superconducting volume fraction of the samples and we will justify this assignment in the following discussion.

In order to examine the effect of the sample size, the sintered specimens were crushed into powder. The particle diameter was 1–4 μm from SEM observation. Figure 6 shows the temperature dependence of the shielding and Meissner signals for the powdered samples under an applied field of 0.2 Oe. Compared to Fig. 4, it is obvious that the reversibility of the magnetization curve of the powdered samples is much higher than that of the sintered bulk specimens, as has been predicted based on the pinning model.[10,13,14] Furthermore, it should be noted that the observed Meissner fraction increases as the sample is crushed into powder while the shielding fraction decreases. We assume the decrease in the shielding signal of the powder to be due to the particle size being as small as the penetration depth λ. Even in the absence of vortex

penetration, the magnetic field can penetrate into the surface over a distance λ. Since λ is inversely proportional to the square root of carrier concentration, it should become shorter with increasing Sr context x. One then expects that the decrease in the volume fraction due to field penetration should be more significant in the underdoped region than in the overdoped region. This is indeed noticed in Fig. 7, where volume fractions estimated from data of Fig. 6 are plotted.

In order to examine the effect of surface penetration of the magnetic field, we evaluated λ, following Fetter[21] and Sheilling, Hulliger, and Ott[22] from the isothermal magnetization curves in the field range $H_{c1} < H_a < H_{c2}$ and at temperatures high enough that the pinning of the flux lines can be neglected. For the isothermal reversible magnetization,

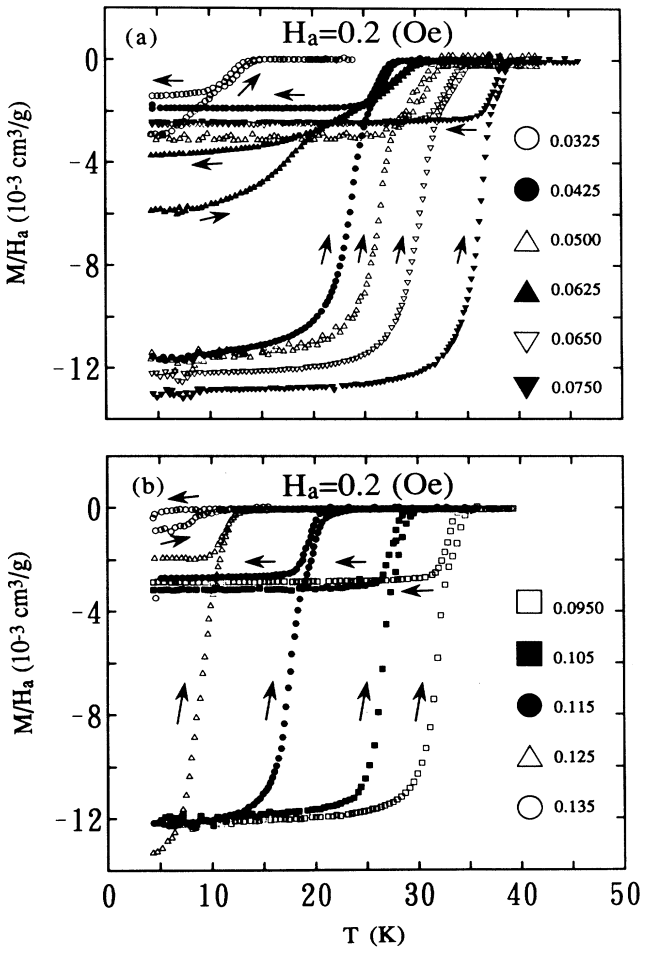

FIG. 4. Meissner and shielding curves of sintered spray-dried–slow-cooled samples ($8.0\times1.5\times0.5$ mm) under $H_a=0.2$ Oe in (a) the underdoped region and (b) overdoped region. The perfect diamagnetism line of -1.14×10^{-2} cm^3/g for $x=0.075$. The deviation of the onset temperature of cooling and warming curves at elevated temperatures is due to the instrumental hysteresis.

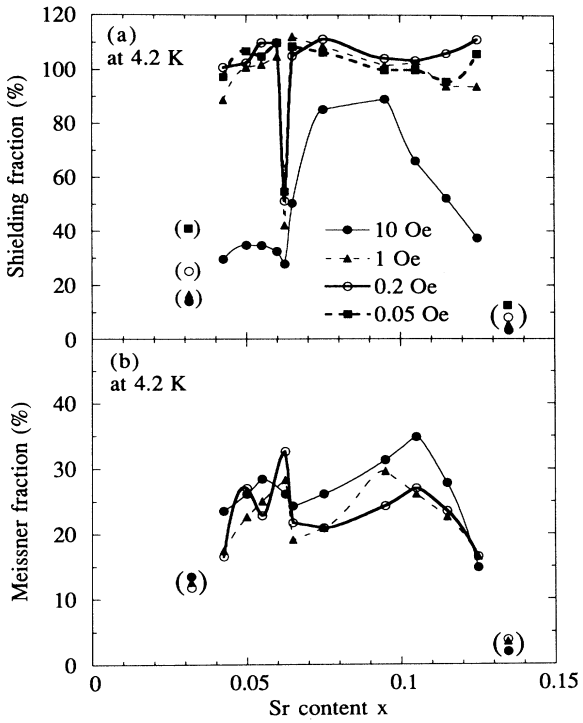

FIG. 5. Apparent superconducting volume fractions estimated for bulk sintered samples by (a) the shielding and (b) the Meissner signals at 4.2 K under $H_a=10,1,0.2$, and 0.05 Oe. The data points for $x=0.0325$ and 0.135 are shown in brackets because the T_c for these samples are judged too low for this estimation.

$$\frac{\partial M}{\partial \ln H}=-\frac{\phi_0}{64\pi^2\lambda^2}g(\gamma)\,,$$
$$g(\gamma)=\gamma^{-1/3}\{\gamma+(\gamma^2-1)^{-1/2}\ln[(\gamma^2-1)^{1/2}+\gamma]\}\,, \tag{1}$$

where $\lambda=(\lambda_{ab}^2\lambda_c)^{1/3}$ and γ is the anisotropic factor. The magnetization was measured at several fields from 0.1 to 1 T for powdered samples. It had a reversible region for the samples with $x\le0.105$. Because the reversible magnetization range became narrower as x increased, the estimation of the λ value was limited to $x\le0.095$. In Fig. 7(a), the obtained penetration depth is plotted by the dotted curve in $\lambda(0)$, estimated according to the two-fluid model,

$$\lambda(T)=\lambda(0)(1-t^4)^{-1/2}\quad(t=T/T_c)\,. \tag{2}$$

We adopted the anisotropy parameter $\gamma=15$ at $x=0.075$ from the torque magnetometry[23–25] and the variation of γ with x was estimated from the resistivity results in Ref. 26. The estimated value of $\lambda(0)$, for example, at $x=0.075$ was 790 nm. This is of comparable size to the grain radius. Therefore, the shielding signal is expected to be significantly reduced even if the specimen powder is 100% superconductive. The penetration depth was found to decrease monotonically with Sr content x. This essentially explains why the diamagnetic signals, both

Meissner and shielding, increasing with x as in Fig. 7.

It is noted in Fig. 7 that nearly the same volume fraction is obtained for the powdered samples both by Meissner and shielding measurements. This clearly tells us that the different fractions obtained in Fig. 5 for bulk samples are due to the pinning effect. This is further evidenced by the increase in the Meissner fraction when the bulk samples are crushed into powders as seen in Figs. 5(b) and 7(b) in the overdoped compositional region. In the smaller sized sample, the exclusion process can take place readily because of the shorter length required for the flux escape.

In the case of the bulk sample, the penetration depth λ is negligible compared with sample size. But in the case of the powdered sample of which the average grain size is about 2 μm, the λ values obtained cannot be neglected anymore. Roughly speaking, penetration depth of 1 μm should reduce the volume fraction to less than 50% even if the sample is wholly superconductive. This is exactly seen in Figs. 5(a) and 7(a), when the shielding signals are compared. It is then readily understood why both the Meissner and shielding signals increase as the penetration depth decreases with Sr doping in the case of powdered samples. This is in contrast to the case of the bulk samples in which the shielding signal is always nearly 100% unless the T_c is very low ($x=0.0325$ and 0.135).

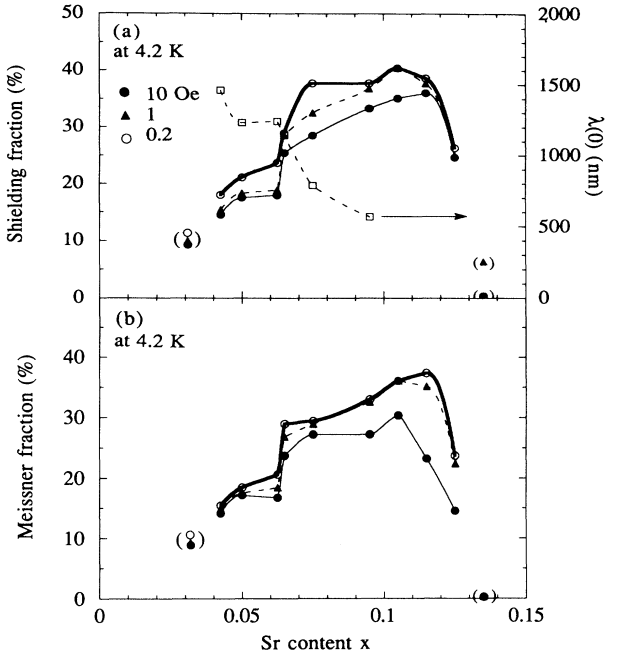

FIG. 7. Apparent superconducting volume fraction for powdered samples estimated from (a) the shielding and (b) Meissner signals at 4.2 K under $H_a=10,1$, and 0.2 Oe. The penetration depth $\lambda(0)$ as estimated from the reversible magnetization is also shown by the open square symbols. As in Fig. 5, the values at the compositions with very low T_c are shown in the brackets.

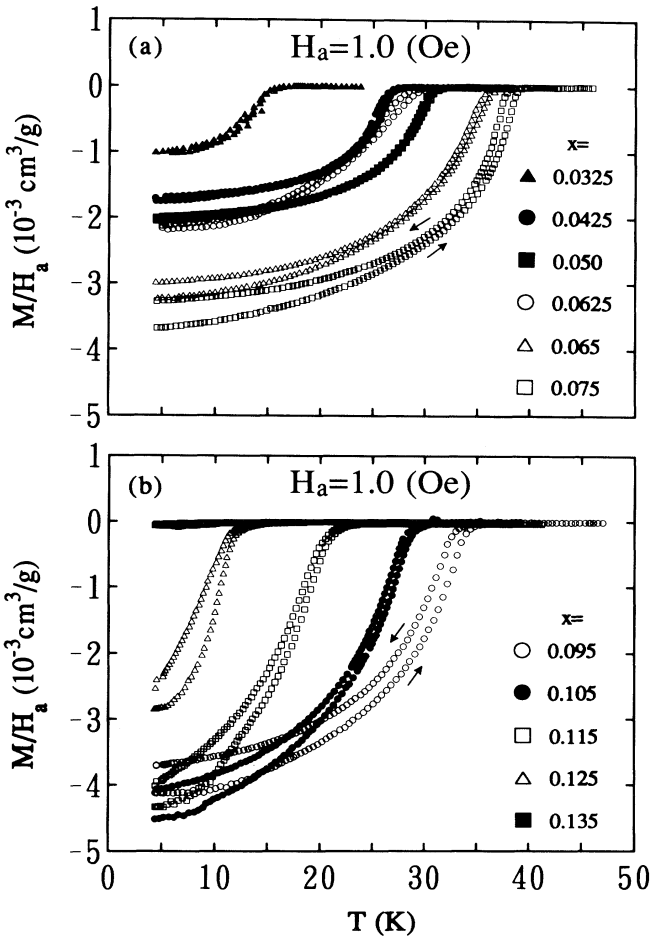

FIG. 6. Meissner and shielding curves for crushed powder samples under $H_a=1$ Oe in (a) the underdoped and (b) the overdoped regions. Note that the curves are much more reversible for each composition than the case for bulk sintered samples given in Fig. 4. The particle size is 1–4 μm from SEM observation.

The above arguments lead us to conclude that all the samples with T_c high enough relative to 4.2 K, the lowest achievable temperature of the experiment, are essentially 100% superconductive. In order to demonstrate the 100% superconductivity of samples of composition in the overdoped region (tetragonal phase), we have performed similar Meissner and shielding signal measurements on a single crystal of composition $x=0.12$, grown by the traveling solvent–floating zone method, details of which are given in Ref. 26. As seen in Fig. 8, both the Meissner signal at the lowest field and the shielding signal indicate nearly 100% superconductivity of the sample.

In the single crystal, the effect of pinning during the Meissner exclusion process of vortices can be lessened by lowering the applied field intensity as has been advocated by Malozemoff *et al.* and ourselves.[8–14] Indeed, the Meissner fraction reaches nearly 100% for the single crystal with $x=0.12$. On the other hand, in the powdered samples, the pinning effect is reduced because of the small particle size. The Meissner and shielding curves should be similar to each other as observed in

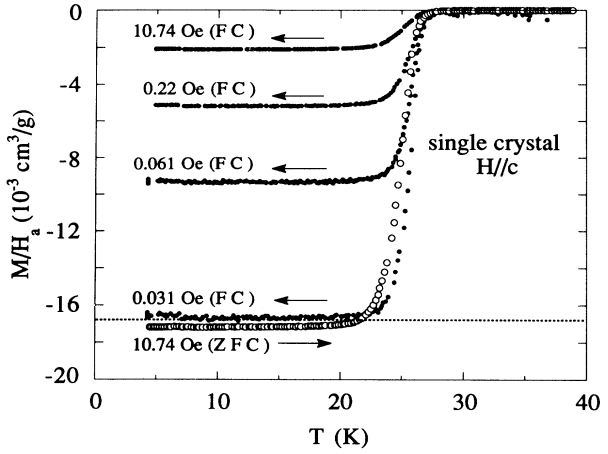

FIG. 8. Shielding the Meissner curves for the single-crystal specimen of LSCO with $x=0.12$ under various magnetic-field intensities. The dotted line shows the 100% diamagnetic level considering the demagnetization factor (Ref. 27) ($\cong 0.317$) estimated for the specimen size 3.55 (a axis)$\times$1.27 (c axis)$\times$0.70 (b axis) mm^3. The field was applied along the c axis.

Figs. 6(a) and 6(b). Instead, however, one has to take the penetration depth into account when it is comparable to the particle size. This explains why both the Meissner and shielding fractions are significantly lower, especially in the underdoped region, where λ becomes longer. In the sintered body, the shielding fraction should be perfect as long as the field intensity is lower than the effective H_{c1} at the polycrystalline grain boundaries. From Fig. 5(a), one can estimate the effective H_{c1} to be between 1 and 10 Oe. The Meissner fraction, however, is determined by the pinning and penetration effects. Hence, the interpretation of the Meissner fraction obtained on sintered samples should be subjected to a greater ambiguity.

Based on the Meissner measurements of sintered bulk samples, Takagi *et al.*[15] claimed a significant decrease in the superconducting volume fraction at $x \geq 0.105$ and concluded that superconductivity is absent beyond the orthorhombic-to-tetragonal phase boundary. Also, in the present observation in Fig. 5(b) it is seen that the Meissner fraction does decrease beyond this composition in the bulk samples. In the powdered samples, however, the Meissner fraction continues to increase even beyond $x=0.105$ into the tetragonal phase region, clearly indicating that the tetragonal phase is still a bulk superconductor. In order to make sure that our samples prepared by the spray-drying method also undergo the orthorhombic-to-tetragonal phase transition, we performed detailed x-ray-diffraction measurements as shown in Fig. 9. In Fig. 9(a) the peaks (040) and (400) in the orthorhombic notation and (220) in the tetragonal notation are shown for various compositions and in Fig. 9(b) the FWHM of each peak was plotted through this structural phase boundary. The results clearly indicate that the system is orthorhombic at 10 K in the compositional region $x \leq 0.095$, but is tetragonal at $x \geq 0.105$. It should be

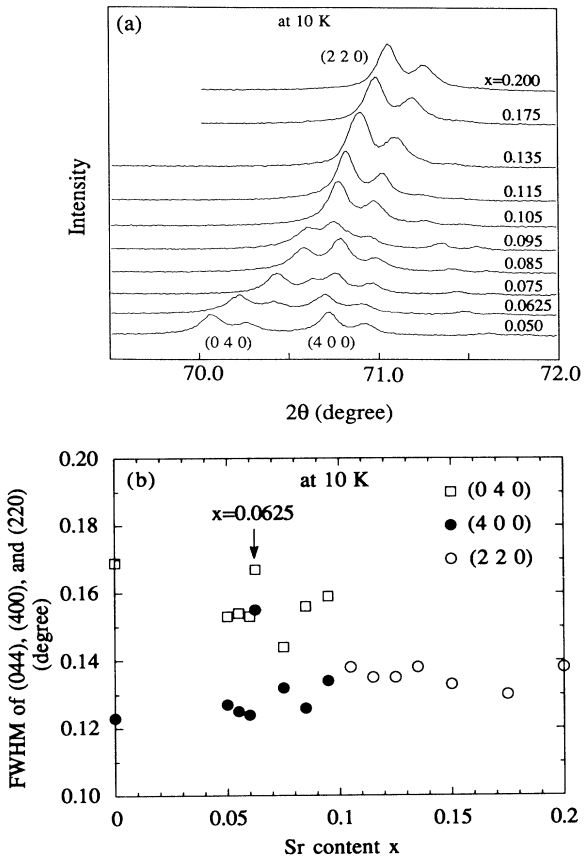

FIG. 9. XRD profiles of the orthorhombic (040) and (400), and the tetragonal (220) peaks (a) at 10 K, and (b) the FWHMs of the three peaks. Above the composition $x=0.105$, the two orthorhombic peaks (400) and (040) merge into tetragonal (220) while the FWHM remains almost constant, indicating the absence of the orthorhombic phase above $x=0.105$.

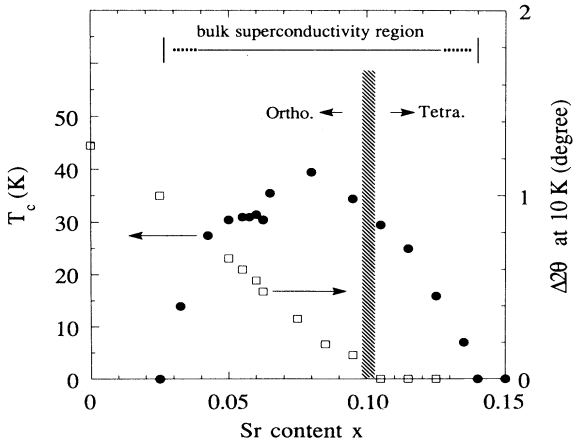

FIG. 10. Orthorhombic splitting (400)–(040) at 10 K (squares), T_c (solid circles), and the bulk superconductivity region in the $(La_{1-x}Sr_x)_2CuO_{4-\delta}$ system.

noted that the FWHM stays nearly constant in the overdoped region ($x \geq 0.105$) at 10 K suggesting the absence of structural inhomogeneities in this region. Furthermore, the anomalous increase in the FWHM was observed only at $x = 0.0625$, where the shielding fraction showed an anomalous dip [Fig. 5(a)].

Figure 10 summarizes the structural phase boundary, T_c and the bulk superconductivity region. The result for the structural phase transition is in good agreement with the observation by Takagi *et al.*[15] Here orthorhombicity is expressed by the angle splitting $\Delta 2\theta$ between the (040) and (400) peaks. The superconductivity region indicated here should be regarded as the narrowest bound which is judged by the measurements down to 4.2 K. This bound may be further extended by a lower temperature study.

IV. CONCLUSION

With the aid of a spray-drying–slow-cooling process, we were able to prepare a homogeneous solid-solution system of $(La_{1-x}Sr_x)_2CuO_{4-\delta}$ which was judged to be 100% bulk superconductive over a wide compositional region, at least $0.0425 \leq x \leq 0.125$, except for the composition of anomaly at $x = 0.0625$. The superconducting region extends over both orthorhombic and tetragonal phases across the boundary. The orthorhombicity, therefore, is not a necessary condition for the occurrence of superconductivity. It was shown that a systematic examination is needed in order to judge the superconductivity volume fraction from Meissner and shielding measurements, taking into account the effects due to vortex pinning as well as London penetration.

ACKNOWLEDGMENTS

This work was supported by a Grant-in-Aid for Scientific Research on Priority Areas, "Science of High Tc Superconductivity" given by the Ministry of Education, Science, and Culture of Japan. The single crystal of LSCO was kindly provided by T. Kimura of the Univ. of Tokyo. We also thank Dr. D. Pooke for helpful discussions.

[1]K. Kishio, K. Kitazawa, N. Sugii, S. Kambe, K. Fueki, H. Takagi, and S. Tanaka, Chem. Lett. **1978**, 635 (1978).

[2]J. B. Torrance, A. Bezinge, A. I. Nazzal, and S. S. P. Parkin, Physica C **162-164**, 291 (1989).

[3]J. D. Jorgensen, P. Lightfoot, S. Pei, B. Dabrowski, D. R. Richards, and D. G. Hinks, in *Advances in Superconductivity III,* Proceedings of the 3rd International Symposium on Superconductivity, edited by K. Kajimura and H. Hayakawa, Sendai, 1990 (Springer-Verlag, Berlin, 1991), p. 337.

[4]K. Yoshimura, Y. Nishizawa, Y. Ueda, and K. Kosuge, J. Phys. Soc. Jpn. **59**, 3073 (1990).

[5]R. B. Van Dover, R. J. Cava, B. Batlogg, and E. A. Rietman, Phys. Rev. B **35**, 5337 (1987).

[6]P. Lightfoot, D. R. Richards, B. Dabrowski, D. G. Hinks, S. Pei, D. T. Marx, A. W. Mitchell, Y. Zheng, and J. D. Jorgensen, Physica C **168**, 627 (1990).

[7]K. Yoshimura, T. Imai, T. Shimizu, Y. Ueda, K. Kosuge, and H. Yasuoka, J. Phys. Soc. Jpn. **58**, 3057 (1989).

[8]A. P. Malozemoff, L. Kurusin-Erubaum, D. C. Cronemeyer, Y. Yeshurun, and F. Holtzberg, Phys. Rev. B **38**, 6490 (1988).

[9]K. Kitazawa, O. Nakamura, T. Matsushita, Y. Tomioka, N. Motohira, M. Murakami, and H. Takei, in *Advances in Superconductivity II,* Proceedings of the 2nd International Symposium on Superconductivity, edited by T. Ishiguro and K. Kajimura, Tsukuba, 1989 (Springer-Verlag, Berlin, 1990), p. 609.

[10]K. Kitazawa, T. Matsushita, O. Nakamura, Y. Tomioka, N. Motohira, T. Tamura, T. Hasegawa, K. Kishio, T. Tanaka, and H. Kojima, in *Proceedings of the International Conference of Superconductivity, Bangalore (India) 1990, edited by S. K. Joshi, C. N. R. Rao, and S. V.* Subramanyam (World Scientific, Singapore, 1990), p. 241.

[11]N. Bontemps, P. Monod, and P. Regnier (unpublished).

[12]D. Wohlleben, G. Michels, and S. Ruppel, Physica C **174**, 242 (1991).

[13]T. Matsushita, E. S. Otabe, T. Matsuno, M. Murakami, and K. Kitazawa, Physica C **170**, 375 (1990).

[14]L. Krusin-Elbaum, A. P. Malozemoff, D. C. Cronemeyer, F. Holtzberg, John R. Clem, and Zhidong Hao, J. Appl. Phys. **67**, 4670 (1990).

[15]H. Takagi, R. J. Cava, M. Marezio, B. Batlogg, J. J. Krajewski, W. F. Peck, Jr., P. Bordet, and D. E. Cox, Phys. Rev. Lett. **68**, 3777 (1992).

[16]K. Kishio, J. Shimoyama, T. Hasegawa, K. Kitazawa, and K. Fueki, Jpn. J. Appl. Phys. **27**, L1229 (1987).

[17]M. Suzuki and M. Hikita, Jpn. J. Appl. Phys. **28**, 1368 (1989).

[18]S. Mitra, J. H. Cho, W. C. Lee, D. C. Johnston, and V. G. Kogan, Phys. Rev. B **40**, 2674 (1989).

[19]A. R. Moodenbaugh, Y. Xu, M. Suenaga, T. J. Folkers, and R. J. Shelton, Phys. Rev. B **38**, 4596 (1988).

[20]J. D. Axe, A. H. Moudden, D. Houlwein, D. E. Cox, K. M. Mohanty, A. R. Moodenbaugh, and Youwen Xu, Phys. Rev. Lett. **62**, 2751 (1989).

[21]A. L. Fetter, Phys. Rev. **147**, 153 (1966).

[22]A. Sheilling, F. Hulliger, and H. R. Ott, Physica C **168**, 272 (1990).

[23]B. Janossy, H. Kojima, and L. Fruchter, Physica C **176**, 517 (1991).

[24]D. E. Farrell, C. M. Williams, S. A. Wolf, S. A. Bansal, and V. G. Kogan, Phys. Rev. Lett. **61**, 2805 (1988).

[25]V. G. Kogan, Phys. Rev. B **24**, 1572 (1981).

[26]T. Kimura, K. Kishio, T. Kobayashi, Y. Nakayama, N. Motohira, K. Kitazawa, and K. Yamafuji, Physica C **192**, 247 (1992).

[27]J. A. Osborn, Phys. Rev. **67**, 351 (1945).